

DEVELOPMENT OF INDUSTRIAL SHEET METAL FORMING PROCESS USING COMPUTER SIMULATION AS INTEGRATED TOOL IN THE CAR BODY DEVELOPMENT

Gleiton Luiz Damoulis

Dept. de Engenharia Mecatrônica e de Sistemas Mecânicos - Escola Politécnica da Universidade de São Paulo – Av. Prof. Mello Moraes, 2231 – 05508.900 S. Paulo – SP – gleiton.damoulis@volkswagen.com.br

Gilmar Ferreira Batalha

Laboratório de Engenharia de Fabricação – Dept. de Engenharia Mecatrônica e de Sistemas Mecânicos - Escola Politécnica da Universidade de São Paulo – Av. Prof. Mello Moraes, 2231 – 05508.900 S. Paulo – SP. gfbatalh@usp.br

Abstract: *Successful industrial applications of the explicit finite element simulation of crash events in the automotive industry triggered a similar demand for the simulation of the stamping process of thin walled components cars are made of. In the car body development the design of body panels and production of tools as well, can be supported effectively by the simulation of the sheet metal forming process with the finite element method (FEM). This paper describes how an explicit finite element program has been applied to lay out industrial deep drawing processes, accomplished by optimization of the methodology, the integration into the development and the updating procedure for the model data and the computational process. The main part of the paper discusses the simulation results and explains the influences of the process parameters (i.e. lubrication conditions and blank holder/ punch force), sheet size and the shape of reverse draw. Finally it is explained how the parameters and geometry were modified to achieve good results*
Keywords: *Sheet metal, forming, friction, simulation*

1. INTRODUCTION

Vehicle Body-in-white is usually complex geometry, irregular pressed parts. Forming these plates is normally a combination of stamping, stretch forming and bending. A detailed analysis and judging of the forming process with conventional processes requires a lot of energy for most cases. Process simulation in the forming technique with the Finite Element Method (FEM) is an efficient and low-cost tool for simulation of the forming process before tool production. During all stages of the forming process the simulation enables a detailed judging of the forming material, the optimal tool form and the process control. The FEM development level nowadays is very high. A variety of effects such as plastically orthotropy and strain rate dependence of the material as well as different friction conditions in the contact area sheet-tool, are describable and corresponding friction conditions are put at disposal by the programs. The user has the task to put in a whole string of parameters for each describable effect. Determination of these parameters requires difficult and special experimentations must be carried on. The present investigation wants to demonstrate which degree of agreement can be achieved between analysis and test. With FEM-Simulation the following can be determinate:

- Forming geometry and sheet drawing-in
- Sheet thickness distribution
- Equivalent plastics strains
- Material flow
- Punch and holder force
- Failure (tearing and wrinkling)

The consequent use of stamping simulation enables:

- Quality improvement of stamping parts by means of optimization of the drawing process, process parameter, material choice, blank and forming steps.
- Saving of development time by means of securing the development course and to reduce costs

2. EXPLICIT FINITE ELEMENT ANALYSIS

2.1 Basic Features

The calculations have been performed with the FEM program PAM-STAMP© which can treat complicated geometry with acceptable run times. According to A.N. Heath et al (1993) [1], the equations systems are integrated in an explicit-dynamic method which, in contrast to an implicit approach, does not involve the solution of complex coupled non-linear equations. Together with robust algorithms, the penalty K based contact is of a one sided searching master-slave type (fig.1)) and contact damping C proportional to the relative velocity of both contact areas, that allows complex problems with many elements to be treated efficiently and reliably. The simulation of metal forming process is one of the major challenges for non-linear FE-Analysis, as all non-linearity concerning geometry with large rotations and large displacements, material with large strains and contact with friction are involved in a large extend.

2.2 The Speed Issue

According to Haug et al (1991) [2], a potential drawback with explicit solutions is their inherent incapacity to furnish one-shoot static solution to structural problems. This is due to the fact that explicit methods operate on the dynamic equation

$$M\ddot{x} = F \quad (1)$$

Where M is the (diagonal) mass matrix, \ddot{x} is the acceleration in the structural degrees of freedom and F are internal resisting forces and external loads. Together with the conditionally stable central difference dynamic solution algorithm, velocity and displacements can be calculated at discrete time intervals, the stable step size of which depends on the smallest travel time of elastic stress waves between points of a discrete model (speed of sound in the material). Typical car crash FE-Models yield stable time steps of the order of one microsecond and a 100 millisecond crash simulation may require up to 100.000 solution time steps. How, then can an explicit dynamic solver be applied efficiently to the relatively slow motion stamping process? The answer is that in most practical cases the punch velocity can safely be increased by substantial factors without the inertia effects of the moved sheet particles to significantly affect the results. Preliminary investigations showed that punch velocities might reach 15-20 meters per second and more, before the effect of inertia will have an influence in the principal stamping results. It is thus feasible to drive stamping simulations at somewhat higher velocities than real, when only velocity dependent or rate effects are calculated, based on the true punch velocity.

2.3 Ramping and Damping

Another simple means to reduce unwanted inertia effects is to apply loads and punch velocities not suddenly, but by ramping up the load with carefully chosen functions of time, thus reducing spurious high frequency response effects from the outset. Judicious application of internal and external damping can also reduce such effects and can lead to stable quasi-static asymptotically solutions.

3. CONTACT AND FRICTION

Among the most important enhancements in a crash simulation program needed for the successful simulation of stamping processes, are the adequate descriptions of the material behavior and the complex contact/friction phenomena between the blank (sheet) and the tools (punch, blank holders and dies). Basic Coulomb friction will not adequately describe the dependence of the friction coefficients on normal pressure, sliding velocity etc. Popular *Penalty* contact algorithms may neither be robust and accurate for enough to yield stable and accurate normal contact pressures, and had to be modified to add damping terms for stability and tributary area calculation for accurate output of normal pressures. For only if the calculated normal pressure is accurate and stable, will the added precision built into the laws of friction be of any use. Contact between the tools and sheet is identified with efficient search algorithms. Contact forces are calculated with a penalty force method that is equivalent to the mechanical system showed in the figure 1. An improvement in this algorithm is the consideration of the correct area surrounding each penetrating node, which results in more exact calculated contact pressures along the edges and non-uniform meshes. Additionally the algorithm was refined to consider the current thickness, which allows the pressure build up caused by blank thickening to be simulated.

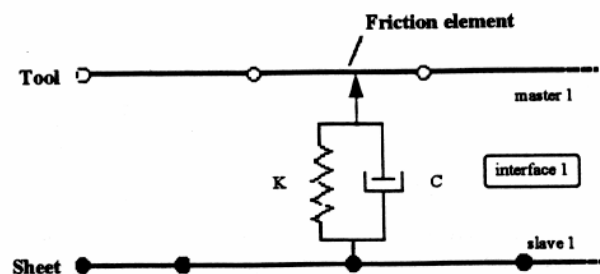


Figure 1. Mechanical equivalent contact force algorithm

The penalty algorithm is robust and can treat complex friction laws without difficulty. At present the program provides both Coulomb friction and an interface for defining general laws of the form $\mathbf{m} = f(\mathbf{S}_n, v)$, with friction coefficient \mathbf{m} , normal pressure \mathbf{S}_n and sliding velocity v .

3.1 Friction Laws

When an accurate description of material behavior appears necessary for successful stamping simulation an accurate description of the friction phenomena is equal importance, because the nature of the tangent forces created by friction between the blank and the tools may be the decisive factor for the manufacturability of a stamped component [3-7]

Friction laws relate a tangent contact stress \mathbf{t} , to normal contact pressures, via a friction coefficient \mathbf{m} which may also depend on contact normal pressure \mathbf{S}_n and the tangent sliding velocity \mathbf{v} and on the lubricant, the temperature, the sliding distance, the sliding direction and the sheet deformation, according to:

$$\mathbf{t} = \mathbf{m} \cdot \mathbf{S}_n \quad (2)$$

In principle $\mathbf{t} = 0$ for $\mathbf{S}_n = 0$ except in simplified draw bead simulation with equivalent planar friction, where:

$$\mathbf{t} = \mathbf{t}_b + \mathbf{mS}_n \quad (3)$$

Being the sliding resistance \mathbf{t}_b created through the bending resistance of the sheet under the bead. Also $\mathbf{t} = \mathbf{t}_y$ yield stress in shear and $\mathbf{m} = 0$ when $\mathbf{S}_n \rightarrow \infty$.

4. MATERIAL LAWS

The material of the sheets is usually highly ductile steel, which is rendered anisotropy, owing to the cold work during the rolling process or owing pre-stresses. According to Hill [8] the anisotropy plasticity can either be considered stationary (*von Mises / Hill criteria*) or evolutionary (e.g., ICT Isotropy Center Translation Theory [9]). Both formulations are incorporated into the program code and outlined below, as well as simple work hardening and strain rate assumptions.

4.1 Von Mises and Hill Type Plasticity Laws – Orthotropy Yield Function

If the sheet material is assumed to exhibit planar and normally orthotropy plastic behavior, then the yield function for plane stress states can be expressed as a *Hill* type criterion as follows:

4.1.1 Orthotropic Material

$$F(\mathbf{s}_{22} - \mathbf{s}_{33})^2 + G(\mathbf{s}_{33} - \mathbf{s}_{11})^2 + H(\mathbf{s}_{11} - \mathbf{s}_{22})^2 + 2L\mathbf{s}_{23}^2 + 2M\mathbf{s}_{31}^2 + 2N\mathbf{s}_{12}^2 = 2Y^2 \quad (4)$$

i) *Hill* Coefficient for *Lankford* ratio=0:

$$\mathbf{s} = \frac{1}{\sqrt{2}} [2(2 + F - G)\mathbf{s}_{22}^2 + 2\mathbf{s}_{11}^2 - 2(2 - G)\mathbf{s}_{11}\mathbf{s}_{22} + N\mathbf{s}_{12}^2]^{1/2} \quad (5)$$

ii) *Hill* Coefficient for *Lankford* ratio=1

$$\mathbf{s} = \frac{1}{\sqrt{P(R+1)}} [R(P+1)\mathbf{s}_{22}^2 + P(R+1)\mathbf{s}_{11}^2 - 2RP\mathbf{s}_{11}\mathbf{s}_{22} + (2Q+1)(R+P)\mathbf{s}_{12}^2]^{1/2} \quad (6)$$

4.1.2 Normal Anisotropy Material (*Lankford* > 0)

$$\mathbf{s} = \frac{1}{\sqrt{RL+1}} [(RL+1)(\mathbf{s}_{22}^2 + \mathbf{s}_{11}^2) - 2RL\mathbf{s}_{11}\mathbf{s}_{22} + (2Q+1)(R+P)\mathbf{s}_{12}^2]^{1/2} \quad (7)$$

Where:

$$\text{Lankford} = RL = \frac{1}{n} \sum_{i=1}^n RLi \quad (8)$$

4.1.3 Normal Isotropy Material (*Lankford* = 0)

$$\mathbf{s} = [(\mathbf{s}_{22}^2 + \mathbf{s}_{11}^2) + (\mathbf{s}_{11} + \mathbf{s}_{22})^2 + 3\mathbf{s}_{12}^2]^{1/2} \quad (\text{Von Mises}) \quad (9)$$

4.2 Isotropy behavior: Lankford ratio=0

Where 1,2 and 3 are the axial, transverse and normal directions of a test coupon cut out at a angle \mathbf{a} with respect to the rolling (or pre stress) direction; P,Q and R are *Lankford* coefficients, where $r_a = \mathbf{e}_{22}(\mathbf{a}) / \mathbf{e}_{33}(\mathbf{a})$ for angles $\mathbf{a} = 90^\circ, 45^\circ, 0^\circ$ respectively, which are determinate by a multi-axial tension test; \mathbf{e}_{22} and \mathbf{e}_{33} are experimentally measured transverse and normal (plastic) strains; $\mathbf{s}_{11}, \mathbf{s}_{12}$ and \mathbf{s}_{22} are in plane normal and shear stresses of the material, (F, G, H, L, M, N) are constant parameters and \mathbf{s}_{ij} is the stress tensor. A plasticity algorithm based on these criterions have been incorporated to the FE-Program, incorporating the additional assumption that Y is a function of the effective plastic strain \mathbf{e}^P with:

$$\mathbf{e}^P = \sqrt{(2/3 \mathbf{e}_{ij}^P \mathbf{e}_{ij}^P)} \quad (10)$$

For the plastic strain tensor, \mathbf{e}_{ij}^P .

The value Y can be defined either thru experimental points or with the *Krupkowski* formula:

$$Y = K(\mathbf{e}^P + \mathbf{e}_0)^n \quad (11)$$

Where K is the hardening factor, \mathbf{e}_0 is the offset strain and n is the hardening exponent in *Krupkowski's* formula. These Material parameters can be obtained through fitting from measured uniaxial stress-strains curves.

4.3 ICT Isotropy Center Translation Plasticity Algorithm

An alternative formation of evaluative orthotropy (or anisotropy) plastic behavior, well adapted to sheet steel material, is the recent phenomenological theory of Isotropy Center Translation. According to Maziliu et al (1990) [9], this theory of anisotropy plasticity, the deviatory invariant of the isotropic yield function translate independently from each other in stress space, producing translations and distortions of the yield surface, following any pre-deformation. The distortion is due to the anisotropy induced by the appearance of texture in the microscopic polycrystalline aggregate. Among historical and recent attempts to elaborate yield surface models, capable of describing rotation and distortion in addition to the growth and translation of the conventional isotropic and kinematics plastic hardening laws, the ICT theory has the advantage of being formulated with direct support of micro plasticity, but in this case it will be necessary to determine 27 material parameters. According to the theory of Isotropy Center of Translation (ICT), the yield function of a cold prestrained metal has the form:

$$f \equiv E(J_a, K_b) - F(L_g) = 0 \quad (12)$$

Here are the parameters J and K proportional to the second and third invariant from the stress tensor $S_{ij} = \mathbf{s}_{ij} - 1/3 \mathbf{d}_{ij} \mathbf{s}_{kk}$ and displaces the independent values \mathbf{a}_{ij} , \mathbf{b}_{ij} and \mathbf{g}_{ij} in the stress field.

$$J_a = (S_{ij} - \mathbf{a}_{ij})(S_{ij} - \mathbf{a}_{ij}) \quad (13)$$

$$K_b = \det(S_{ij} - \mathbf{b}_{ij}) \quad (14)$$

$$J_g = (S_{ij} - \mathbf{g}_{ij})(S_{ij} - \mathbf{g}_{ij}) \quad (15)$$

$$K_g = \det(S_{ij} - g_{ij}) \quad (16)$$

$$\text{Where } L_g = K_g / J_g^{3/2} \quad (17)$$

An algorithm based on these equations has been developed, where $E(J_a, K_b)$ and $F(L_g)$ are assumed to be polynomials. Hardening and strain rate effects are treated analogously to the *Hill* algorithm, i.e. the various *ICT* parameters are treated as functions of e^P and e^P .

5. EXAMPLE OF INDUSTRIAL APPLICATION

Various studies have been performed to evaluate simulation accuracy by comparison with experiment. Considered parts included some simple benchmark geometries (U-profiles, cylindrical, spherical and rectangular dishes) as well as more complicated vehicle body components such as side panels, fenders, door panels and others. Quantities used for comparison were in each case the shape of the deformed sheet, thickness and strain distributions as well as the forming force history.

5.1 Model Discretisation

To perform this calculation, a Side Panel outer from a small car were took and in the critical deep-drawing area (fig.2) a FEM model from the geometry were made. The sheet metal dimension in this case is 250x150mm. For the sheet material a St1405 was defined, which is a usual material for deep-drawing applications in the automotive industry. The material identification data is represented in the tab.1. A contact friction coefficient of 0.1 has been used, according to the *Coulomb's* law (this means that in the reality the part will be drawn with film oil over the sheet) and a equivalent draw bead model has been defined. The chosen loads are 1200 [kN] for the holder and 3000 [kN] for the punch. The tool is considered as a rigid body and it was described as 11048 elements for the die, 1219 elements for the holder and 10023 elements for the punch.

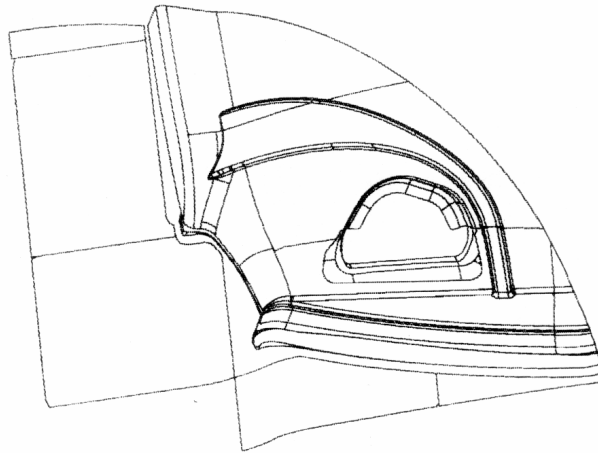


Figure 2. Critical area of a body-in-white side panel outer

To achieve the results, it was decided to perform the calculations in three different forming stages. The first one demonstrates the behavior of the sheet after the contact between die/holder, the second one demonstrates the stamping process until the punch has reached the die top and the third one, which after analysis of the results from forming stage two, we concluded that in some areas we needed a local mesh refinement to improve the local analysis accuracy.

5.2 Forming Stages

To describe the calculation models, the PAM-GENERIS© pre-processor program has been used. It was prepared an offset from the die and holder model (fig.3a). The holder is forced and damped to ground to prevent undesired dynamic oscillations and the holder velocity is increased to a maximum of 10m/s. The sheet initial stage was performed with 16759 shell elements.

For the forming stage 2, after the blank holder action, a second model was prepared with the output date from the stage 1, considering in this model the punch driving into the die (fig.3b). For representation reasons the model (b) is showed opened, but we consider the blank holder in contact with the pre-formed sheet.

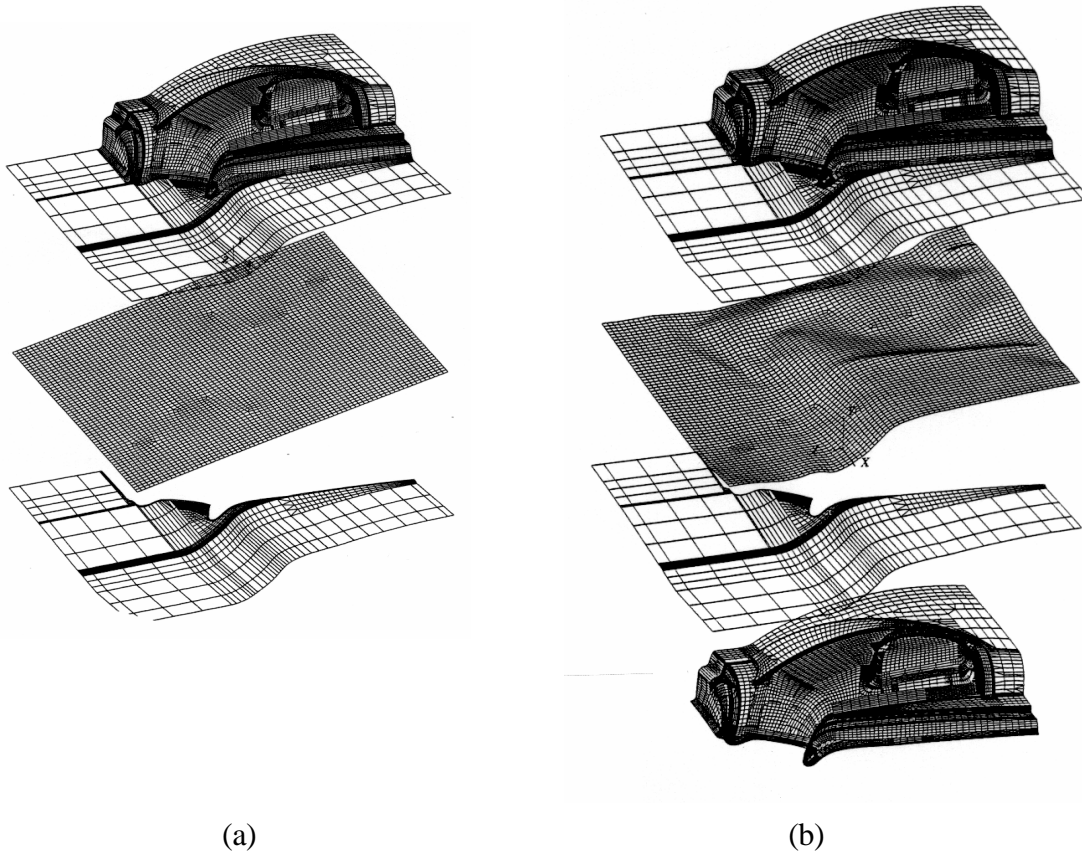


Figure 3. Forming stages 1 and 2 discretization models.

The punch velocity in the stage 2 is increased to a maximum of 10m/s. In this calculation, the automatic mesh refinement program has allowed to the over limit of 30798 elements to perform stage 2. In the area were the large strains were detected we improved the mesh refinement and the same sequence as in step 2 was performed (Forming Step 3). The sheet was refined until 36000 shell elements.

E [GPa]	210
ν	0,30
K	0,5673
e_0	0,0073
n	0,264
Sheet Thickness [mm]	1,00
<i>Lankford Coefficient</i>	
P	1,8
Q	1,5
R	2,3
m_{lb}	0,1

Table 1 - Sheet metal characterization data.

6. SIMULATION RESULTS

Figure 3a exhibit simulation step at the stage 1 (figure 3a). The simulation results demonstrate the simulation capacity to predict the wrinkling of the sheet under the blank holder, owing to low holder pressure. Here we can also see the undesired direction of the pre-formed sheet against the punch that can lead us to an undesired behavior of the sheet inside the tool (we can not forget that this is a surface part, therefore a high level of surface quality is required for painting reasons). In the fig.4 we can evaluate the strains distribution over the part and in the fig.5 the referent forming diagram is displayed to determine the critical points where the plastic strains are over the deformation criteria, this means tendency to tearing points. A very important criterion for this evaluation is the Forming Limit Diagram (FLD), where every finite element with its respective principal strain is represented. All the points over the limit forming represent a tearing point during the drawing process.

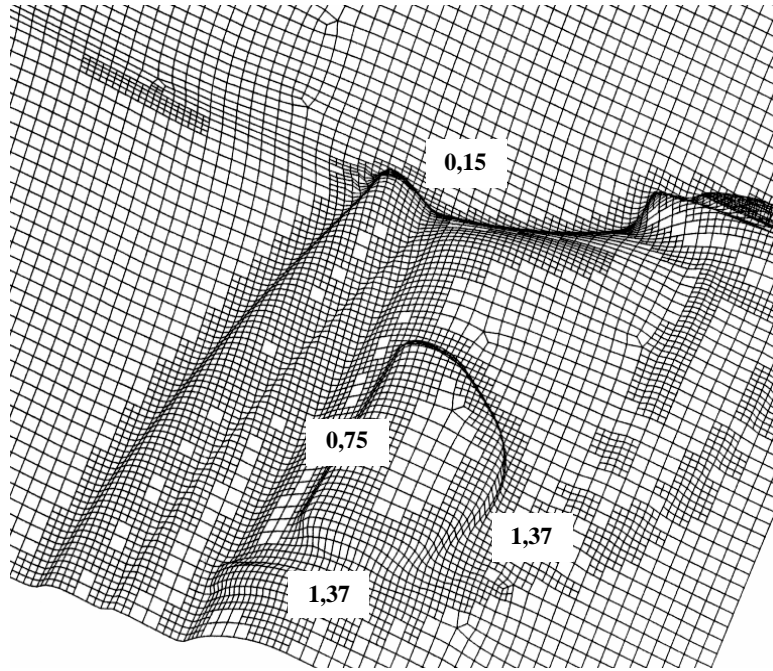


Figure 4 - Strain distribution after deformation in the step 2.

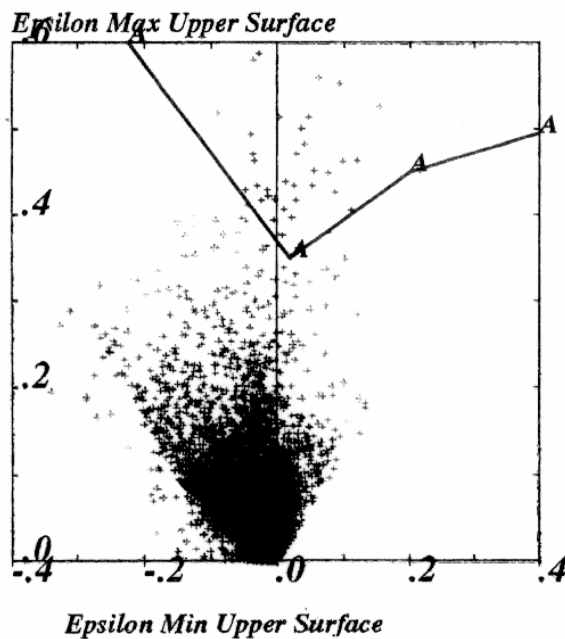


Figure 5 - Forming Limit Diagram.

In the fig. 6 the thickness distribution is displayed. In two areas the minimal thickness decrease under 0.48 mm, what takes a high probability to tear. In these local a mesh refinement will be necessary to improve the local analysis accuracy (step 3, fig.7a).

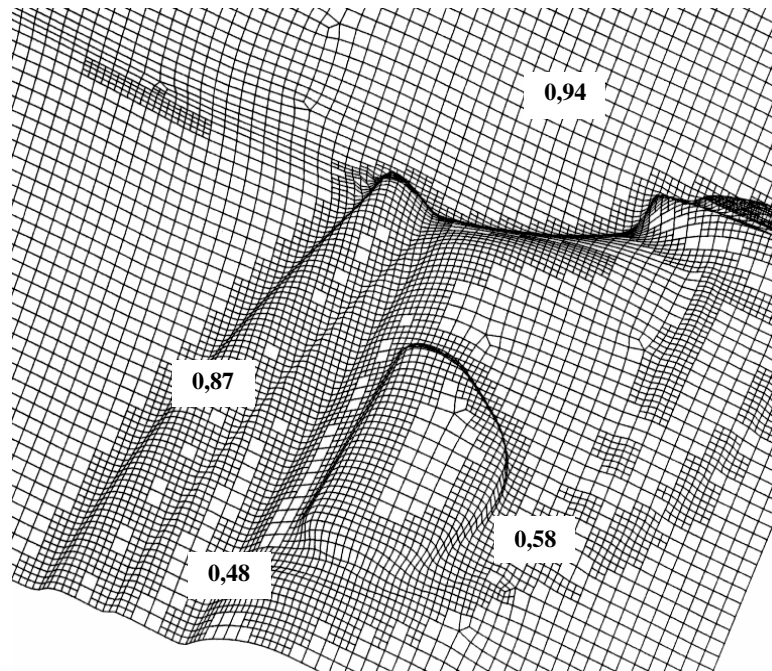


Figure 6. Thickness distribution after deformation in the step 2

Considering the results of the calculation the material flow, thickness distribution and failure in the sheet was in good correspondent with the experimental results. The results show that in a comparison between calculated and experienced results (fig. 7b), in the same critical areas the sheet tearing was founded.

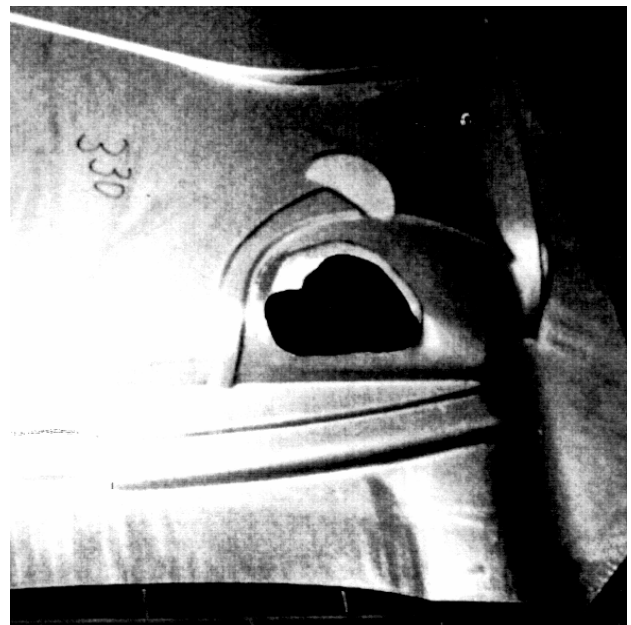
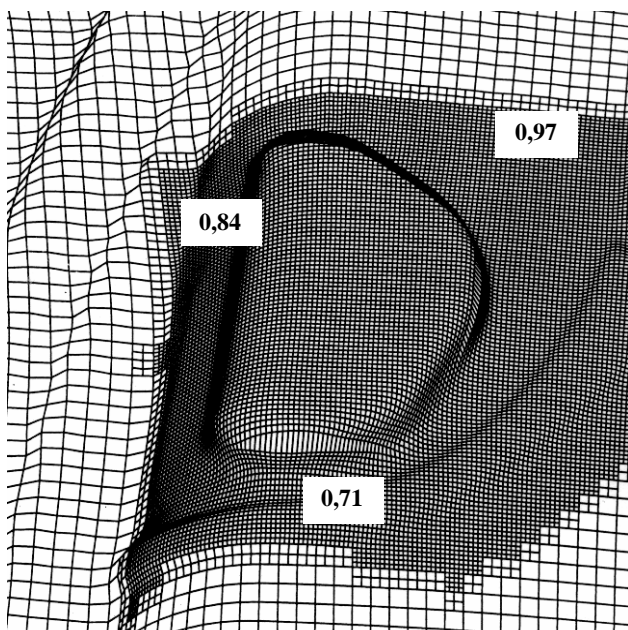


Figure 7 – (a) Thickness distribution after deformation in the step3 (tool radius optimization) and (b) prototype pressed body-in-white part.

8. TOOL OPTIMIZATION

The criterion of a limit shell thickness has been reached, because of the friction coefficient between the punch and the blank has been too high. The modification of the geometry on the critical area can be recommended. In this case a modification of the tool radius (fig.7a) is recommended, in order to improve thickness and strain distribution. After the modifications, a new calculation has been performed. In the critical areas the minimal thickness was calculated to 0,71mm (fig.7a) and wrinkling and tearing (see pressed part fig.7b) may be avoided.

9. CONCLUSION

If we look to the probable future of drawing tool design, the main goal of simulation to improve the process should be:

- Finding the best blank contour,
- Optimization of tool geometry,
- Improving the process by optimizing the material flow,
- Calculate sheet thickness distribution,
- Calculate equivalent plastic strain,
- Indication of failure (tearing and wrinkling).

Working in this way, the deep drawing simulation now can be used for comparative tool optimization and to study the influence of varying process parameters. With more experience using and improving the practical and theoretical models, sheet forming simulation has become a powerful tool to reduce development time, reduce costs and improve quality.

10. REFERENCES

- [1] Heath A.N., Pickett A.K. & Ulrich, D. Development of Industrial Sheet Metal Forming Process Using Computer Simulation, Dedicated Conference on Lean Manufacturing in Automotive Industries, Aachen, Germany, 1993
- [2] Haug E., Pascale E.di, Pickett A.K. & Ulrich, D. ESI: Industrial Sheet Metal Forming Simulation Using Explicit FE-Methods, VDI Bericht Nr. 894, Germany 1991
- [3] Batalha, G. F., 1998, Some aspects of Surface Qualification and its relationship to metal sheet forming, In: Proc.. I Workshop FINEP/RECOPE – Desafios, Experiências e Expectativas no controle da rugosidade de chapas metálicas para a indústria automotiva, 21 de outubro de 1998, Org. EPUSP / FINEP / RECOPE, S. Paulo, ISBN 85-86686-03-4.
- [4] Batalha, G. F. et al. 1999, Proc. II Workshop FINEP-RECOPE – Qualificação de chapas para a indústria automobilística, 17 de abril de 1999, Org. EPUSP / FINEP / RECOPE, S. Paulo, ISBN 85-86686-05-0
- [5] Batalha, G. F. & Stipkovic Filho, M., 2000, Analysis of the contact conditions and its influence on the interface friction in forming processes, In: Metalforming 2000, Pietrzyk et al. (eds), Balkema, Rotterdam, ISBN 90 5809 157 0, pp. 71-7.
- [6] Batalha, G. F. & Stipkovic Filho, M., 2001, Quantitative Characterization of the surface topography of cold rolled sheets – new approaches and possibilities, J. Materials Processing Technology, 113, pp. 732-8.
- [7] Damoulis, G. - Tiefziehsimulation von Karosseriebauteilen mit FEM als ein Hilfsmittel in einem Ingenieurbüro. Diplomarbeit, TH Karlsruhe, Germany 1996
- [8] Hill, R. - A Theory of the Yielding and Plastic Flow of Anisotropic Metals - Proceedings Royal Society. A193, 1948
- [9] Maziliu, L S. & Kurr, J. Anisotropy Evolution by Cold Prestrained Metals Described by ICT-Theory. Journal of Material Processing Technology, Vol.24, pp.303-311, 1990
- [10] Damoulis G. & Kleinhans U. - Simulation of Sheet Metal Forming Using a FEM Program as Integrated Tool in the Car Body Development. V International Mobility Technology Conference and Exhibit, S. Paulo, Brazil 1996

11. Copyright Notice

The authors are the only responsible for the printed material included in this paper.